RSC Advances

PAPER

View Article Online
View Journal | View Issue

Cite this: *RSC Adv.*, 2017, **7**, 39929

Metabolomics reveal the protective effect of Farfarae Flos against asthma using an OVA-induced rat model†

Jing Li,[ab] Wei Gao,[c] Jining Gao,[d] Hong Li,[d] Xiang Zhang,[e] Xuemei Qin[a] and Zhenyu Li *[a]

Received 11th May 2017
Accepted 27th July 2017

DOI: 10.1039/c7ra05340a

rsc.li/rsc-advances

Farfarae Flos (FF) is widely used in china to treat pulmonary disorders such as coughs, bronchitis, tuberculosis and asthmatic disorders. In this study, a ^{1}H NMR based metabolomic approach coupled with biochemical assay as well as histopathological inspection had been employed to study the protective effect of petroleum extracts of FF (PEFF) against OVA-induced asthma using a rat model. Multivariate analysis revealed that 19 of the perturbed endogenous metabolites in the lung could be reversed by PEFF, and MetPA analysis revealed that the anti-asthamtic effect of PEFF was probably related with regulation of arginine and proline metabolism, pyruvate metabolism and D-glutamine and D-glutamate metabolism. The regulatory effect on the cytokines (IL-4, IL-5, IL-13, and IL-17) and serum HO-1 suggested that the anti-asthmatic action of PEFF was also probably related with the balancing of the Th1/Th2 cells and the Nrf2/HO-1 pathway. The results of chemical analysis showed that the sesquiterpenes were present as the major components in PEFF, and further studies are needed to validate the bioactive compounds responsible for the anti-asthmatic effect of PEFF.

1. Introduction

Asthma is a heterogeneous disease, which is diagnosed by respiratory symptoms such as wheezing, shortness of breath, chest tightness and coughing.[1] It is characterized by chronic airway inflammation with high levels of eosinophils, increased mucus production in the bronchioles, and airway hyperreactivity to a variety of specific and nonspecific stimuli. The pathogenesis of asthma is very complex, with immunological factors being the most important.

Previous studies showed that asthmatic patients had an immunity imbalance of Thl/Th2 *in vivo*. The Th2 cells, which secret IL-4, IL-5, and IL-13, are over activated, while the Th1 cells, which secrete the cytokines of interferon-gamma (IFN-γ), are reduced. IFN-γ shows an inhibitory action on IgE production, while the IL-4, IL-5, IL-13 can promote the production of IgE, which can further stimulate the proliferation and activation of eosinophils. The activated eosinophils will secrete a variety of proinflammatory medium and will lead to chronic inflammation of airway.[2–5]

Among the anti-asthmatic medications available, the glucocorticoid anti-inflammatory drugs are the preferred therapeutic for mild to moderate asthma. However, the requirement for daily inhalation with glucocorticoids is often a cause for poor patient compliance, which limited the use of glucocorticoids in asthma therapy.[6] In addition, steroidal anti-inflammatory drugs are not universally effective in all patients although they are the recommended medication for asthma in clinical practice.[7] On the other hand, long-term use of steroidal anti-inflammatory drugs can cause complications such as pneumonia, fracture, hyperglycemia and cataract.[8] Therefore, the research in the new therapeutic agents with high potency to combat inflammation and relieve asthma with fewer adverse effects is presently the focus of many scientists and physicians.

Traditional Chinese Medicine (TCM) showed unique therapeutic effect in the treatment of various diseases, as it had the advantage of little side effect, low cost and low recurring rate. Various plant-derived natural extracts, such as *Pheretima aspergillum*,[9] *Eclipta prostrata* (L.) L,[10] *Mandevilla longiflora*,[11] with anti-inflammatory properties have been tested for potential application in the treatment of asthma.[12] Farfarae Flos (FF), also known as Kuandonghua in China, is derived from the flower buds of *Tussilago farfara* L. (Coltsfoot), which is widely

[a]*Modern Research Center for Traditional Chinese Medicine of Shanxi University, No. 92, Wucheng Road, Taiyuan 030006, Shanxi, People's Republic of China. E-mail: lizhenyu@sxu.edu.cn; Tel: +86-351-7018379*

[b]*College of Chemistry and Chemical Engineering of Shanxi University, No. 92, Wucheng Road 92, Taiyuan 030006, Shanxi, People's Republic of China*

[c]*Department of Otolaryngology, Head & Neck Surgery, The First Hospital Affiliated with Shanxi Medical University, People's Republic of China*

[d]*Shanxi Hospital of Integrated Traditional and Western Medicine, Taiyuan 030000, People's Republic of China*

[e]*The Center for Regulatory Environmental Analytical Metabolomics, University of Louisville, KY 40292, USA*

† Electronic supplementary information (ESI) available. See DOI: 10.1039/c7ra05340a

used to treat pulmonary disorders such as cough, bronchitis, tuberculosis and asthmatic disorders.[13] In addition, the extracts of FF also showed other bioactivities, such as anti-inflammatory,[14] anti-cancer,[15] neuroprotection,[16] and platelet activating factor inhibition.[17] Phenylpropanoids,[18] flavonoids,[19] triterpenoids,[20] sesquiterpenoids[21] and alkaloids[22] constitute the major classes of secondary metabolites in FF. The sesquiterpenes, which were present as the characteristic components in FF, showed obvious anti-inflammatory activities. As inflammation plays an important role in asthma, we speculated that the sesquiterpene extracts of FF may be used for treating asthma.

The present study aimed to evaluate the protective role of petroleum extracts of FF (PEFF) using OVA-induced rats asthmatic model and its underlying mechanism based on a new strategy, which integrating untargeted metabonomics, partial least square regression analysis, MetPA and molecular docking. To our knowledge, this is the first study that deeply assessed the metabolic regulation of PEFF against asthma.

2. Materials and methods

2.1 Chemicals and plant materials

Petroleum ether (60–90 °C), was acquired from Tianjin University Chemical experimental factory (Tianjin, China). Acetonitrile and methanol of chromatographic grade were obtained from Fisher (USA). The sodium 3-trimethylsilyl[2,2,3,3-d_4]propionate (TSP) was obtained from Cambridge Isotope Laboratories Inc (Andover, MA, USA). D_2O was bought from Norell (Landisville, NJ, USA). Analytical grade $Na_2HPO_4 \cdot 2H_2O$ and $NaH_2PO_4 \cdot 12H_2O$ were obtained from Guangfu Fine Chemical Research Institute (Tianjin, China) and Zhiyuan Chemical Reagent Co., Ltd (Tianjin, China), respectively. Phosphate buffer was prepared with $Na_2HPO_4 \cdot 2H_2O$ and $NaH_2PO_4 \cdot 12H_2O$ (0.1 M, pH 7.4), containing 10% D_2O and 0.1 mM L^{-1} of TSP.

Dexamethasone sodium phosphate (DEX) was obtained from Tianjin kingyork group co., sodium chloride, aluminium hydroxide, Tween-80, were purchased from Sigma (St. Louis, Missouri, USA). The IL-4, IL-5, IL-13, INF-γ, Ig-E and HO-1 ELISA Ready-Set-Go!® kits were obtained from Sangon Biotech (Shanghai, China).

FF was obtained from a local drug store authenticated as the buds of *Tussilago farfara* L. by Prof. Xue-Mei Qin, and the voucher specimens (No. KD-34) were deposited in the herbarium of Modern Research Center for Traditional Chinese Medicine of Shanxi University.

2.2 Extract preparation

The dried flower buds (3 kg) of FF were ground to powder, and extracted three times for 60 min with 4 L of petroleum ether (60–90 °C) under ultrasonication, and the combined extract was concentrated under reduced pressure, which yielded 6.5 g of PEFF for the further chemical analysis and animal experiment.

2.3 NMR and LC-MS analysis of PEFF

For NMR analysis, about 50 mg of PEFF was re-dissolved in $CDCl_3$. After centrifuging for 15 min at 13 000 rpm, the supernatant (600 μL) was transferred into a 5 mm NMR tube for NMR analysis. The NMR spectral was measured using zg30 sequence at 298 K on Bruker Avance 600-NMR spectrometer (600.13 MHz proton frequency, Bruker, Germany) equipped with a Bruker 5 mm double resonance BBI probe.

For the further identification of the chemical components in PEFF, LC-MS was also used. PEFF was analyzed on the UHPLC-Q-Exactive-Orbittrap-MS equipment (Thermo Fisher, USA). Thermo Fisher U 3000 system was fitted with a Wasters BEH C18 (2.1 ×100 mm, 1.7 μm) with ESI ion source. The Z-spray ionization source was maintained at 300 °C with spray voltages of 3.5 kV in the positive ionization mode. Additional operating parameters were: capillary temperature 320 °C, lens voltage 55 kPa, mass resolution 70 000, and mass scan range 80–1500 *m*/*z* in the full-scan mode.

A sample containing 0.5 mg mL^{-1} of PEFF in methanol was passed through a 0.22 μm pore size syringe filter, and an aliquot of 5 μL was injected into the column. Elution was performed using a mixture of 0.03% formic acid (solvent A) and acetonitrile (solvent B) at a flow rate of 0.3 mL min^{-1} in the form of a gradient from 70% to 80% B between 0 and 5 min, from 80% to 95% B between 5 and 25 min.

2.4 Experimental animals

8 week-old female RD rats (180–220 g) were purchased from Beijing Vital River Laboratories Co., Ltd. (SCXK (Jing) 2011-0012, Beijing, China). The rats were housed five rats in each laminar flow cabinet under the following conditions, temperature of 20–24 °C, relative humidity 65 ± 10% and maintained on 12 h light–dark cycle, with food and water *ad libitum*.

60 rats were randomly divided into six groups: control group (sensitized and challenged with saline); model group (sensitized and challenged with OVA); three treatment groups (sensitized and challenged with OVA and treated with PEFF). DEX group (sensitized and challenged with OVA and treated with DEX). The procedures employed for OVA sensitization and challenges, as well as the treatment with PEFF were shown in Fig. 1. OVA sensitization was performed twice at an interval of seven days by intraperitoneal injection of a solution containing 1 mg of OVA and 100 mg of aluminum hydroxide in 0.9% saline solution.[23] The PEFF was dissolved in saline with 2% Tween-80 and diluted to a final concentration of 5 mg mL^{-1}, and stored at 4 °C for further use.

The OVA challenge and drug treatment spray for fourteen consecutive days. Control group: challenged with saline (2% Tween-80) only; model group: challenged with OVA only; LD group: challenged with OVA and treated with 0.1 g kg^{-1} of PEFF;

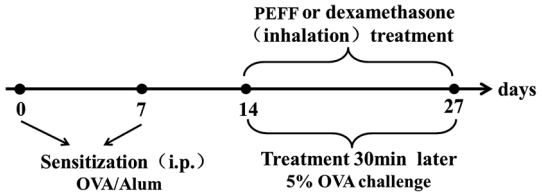

Fig. 1 Rat model of OVA-induced asthma and treatment with dexamethasone and PEFF.

MD group: challenged with OVA and treated with 0.2 g kg^{-1} of PEFF; HD group: challenged with OVA and treated with 0.4 g kg^{-1} of PEFF; DEX group: challenged with OVA and treated with 2 mg kg^{-1} of dexamethasone.

2.5 Collection of serum and bronchoalveolar lavage fluid (BALF)

After the rats were anesthetized with urethane, the blood was collected from the femoral artery and then separated using refrigerated centrifugation at 13 000 rpm for 10 min to afford the serum. The serum samples were snap-frozen in liquid nitrogen and stored at −80 °C for further analysis.

The lungs were lavaged through the tracheal cannula with PBS (pH 7.4), which contain 136.89 mM of NaCl, 2.67 mM of KCl, 8.24 mM of Na_2HPO_4, and 1.76 mM of KH_2PO_4. The airway lumina was washed three times with 1 mL of PBS, then the BALF was collected. The BALF from each rat was pooled, and then centrifuged at 13 000 rpm for 10 min at 4 °C. The cell pellet was resuspended in 1 mL of saline. To perform the leukocyte cell count, cells were identified by HEMAVET950FS automatic animal blood analyzer and classified as eosinophils, lymphocytes, neutrophils, and monocyte.

2.6 Histopathological examination

After BALF collection, the ligated left lung was fixed with 10% (v/v) neutral formalin for 24 h. To enhance fixation, the lungs and tracheas were placed in a rubber-capped ampulla bottle filled to 2/3 maximum volume level with 10% (v/v) neutral formalin. The lung tissues and tracheas tissues were paraffin-embedded, sectioned at 4 μm, and stained with hematoxylin & eosin (H & E) to observe inflammatory cells infiltration in the lung tissues. Images were obtained and studied under light microscopy.

2.7 Determination of biochemical indexes levels

The levels of IL-4, IL-5, IL-13, IL-17, INF-γ, HO-1 and IgE levels in the serum were determined with the corresponding enzyme-linked immunosorbent assay (ELISA) kits according to the manufacturer's instructions.

2.8 Sample preparation of lung tissue for NMR measurement

The right lung (about 600 mg) was extracted with 2700 μL of methanol/water (2 : 1, v/v) using an ultrasonic cell crusher, then was centrifuged at 4 °C and 13 000 rpm for 20 min. The supernatant was dried in nitrogen flow and stored at −20 °C. Then, the dried mass was diluted with 750 μL of phosphate buffer (0.1 M Na_2HPO_4–NaH_2PO_4, pH 7.4) containing 0.1 mM L^{-1} of TSP and 10% D_2O. The mixture was centrifuged at 4 °C and 13 000 rpm for 20 min, and an aliquot of 600 μL supernatant was transferred into 5 mm NMR tubes for ^1H NMR analysis.

2.9 NMR data processing and multivariate analysis

The ^1H NMR spectra were processed using the MestReNova software (version 10.0.1, Mestrelab Research, Santiago de Compostella, Spain). The phase and baseline distortions were corrected manually and referenced to the chemical shift of TSP at 0.00 ppm. Then the spectra were divided and the signal integrals were computed in 0.01 ppm intervals across the region δ 0.5–9.0 ppm. The regions of δ 4.69–5.15 ppm were removed to eliminate the effects of imperfect presaturation of water. Normalization to a total area of all integrals was applied prior to further analysis.

The processed NMR data matrix was imported into Simca-P 13.0 software (Umetrics, Sweden) for multivariate data analysis. Principal component analysis (PCA) was carried out on the mean centered data to obtain an overview and find possible outliers. Partial least squares discriminant analysis (PLS-DA) was applied to determine the differential metabolites between the groups of samples, which were defined as separate response variables. The model qualities were assessed with the total explained variables (R^2X values) and the model predictability (Q^2 values) followed by rigorous permutation tests (number: 200). Orthogonal projection to latent structure-discriminate analysis (OPLS-DA) was also employed to maximize the separation between groups. Potential biomarkers were extracted from *S*-plots constructed with the followed OPLS-DA analysis, and the biomarkers were chosen based on their contribution to the variation. Meanwhile, the underlying relationship between differential metabolites and biochemical indexes was evaluated by PLS-RA. PLS-RA is a multivariate calibration model to reveal the relationship between two matrices (*X* and *Y*) based on the two-block predictive PLS model, which could afford the latent structures of observations by regression.[24] Predicted variations (Q^2Y) and significance of the model (*p* value) are its main diagnostic parameters. In this study, differential biochemical indexes (IL-4, IL-5, IL-13, IL-17, IFN-γ, IgE, HO-1) levels acted as *X*-variables to characterize the asthma. The integrating peak integrals of metabolites acted as *Y*-variables.

To further compare the drug efficacy, efficacy index was calculated with eqn (1), where X_i, M_i, C_i represent relative contents evaluated on the basis of the relative amounts of metabolites from the least-overlapping NMR signals of metabolites in drug-treated groups, model group and control group, respectively.

$$\text{EI (Efficacy index)} = \sum_{i=1}^{n}\left|\frac{X_i - M_i}{C_i - M_i}\right| \times 100\% \quad (1)$$

The relative amounts of metabolites were evaluated by the average peak areas of the least-overlapping characteristic resonances in comparison with that of the internal standard (TSP). Data were expressed as mean ± SEM and *n* presented the number of animals. Statistical analyses were performed using Graph Pad Prism 5.0 software. Analysis of one-way ANOVA analysis was used to compare mean value for the different groups, followed by SPSS 16.0 software for multiple comparisons. A *p* value <0.05 (two-sided) was considered significant.

3. Result

3.1 Chemical analysis of PEFF

The typical ^1H NMR spectrum of PEFF was shown in Fig. S1.† The signals were assigned based on comparisons with the

chemical shift of standard compounds, as well as reported NMR data.[25,26] In addition to the high level of fatty acid or fatty acid ester, the signals corresponding to the doubles bonds and methyl groups of the sesquiterpenoids were obviously detected in the region of δ 4.5–6.5 and δ 0.8–1.2, and the compounds identified by NMR in PEFF were listed in Table S1.†

In addition, LC-MS analysis was also applied, and seven compounds (Fig. S2†) were identified in PEFF (Table S2†). The details of the identification process could be found in the ESI.† The structures of all the identified compounds were shown in Fig. 2. It was obvious that the sesquiterpenoids were present as the major components in the PEFF.

3.2 Pathological examination

H & E staining was applied to investigate the effects of PEFF on lung histological changes in the asthmatic rats. The results indicated that OVA-challenged rats showed marked inflammatory cell infiltration in the peribronchial and perivascular areas as well as airway epithelial thickening. After the treatment of PEFF or DEX, the OVA-induced pathological changes could be significantly attenuated (Fig. 3).

In addition, the results of histological change in the trachea (Fig. S3†) also showed significant tracheal myofibroblast distribution, which reflected the increase of tracheal wall thickness. It is worthy to note that the tracheal wall thickness in the OVA repetitively challenged rats was significantly greater than those in the control animals. The area of enlarged myofibroblast could be reduced significantly after the treatment of PEFF, especially in the HD group, as compared with the rats in the model group.

3.3 Effects of PEFF on inflammatory cell counts in BALF samples

The number of eosinophil, neutrophil, and monocyte in the BALF of OVA-challenged rats were increased significantly as compared with the normal controls. As shown in Fig. 4, after the treatment with the PEFF at all concentrations tested, those increased inflammatory cell counts were reduced significantly in comparison with the model group ($p < 0.01$). In contrast, the number of lymphocyte was reduced in the OVA challenged rats, which could be increased ($p < 0.01$) by the treatment of PEFF as well as the DEX. In addition, microscopic examination of lung sections also confirmed that the migration of inflammatory cells were significantly reduced after the treatment of PEFF in comparison with the model group.

3.4 Determination of biochemical indexes

Several cytokines have been found closely associated with the asthma, such as IL-4, IL-5, IL-13. Thus, the ELISA assay was used to evaluate the changes of these inflammatory mediators in the model and the treatment groups. Sensitisation and challenge with OVA significantly increased ($p < 0.01$) the concentration of IL-4, IL-5, IL-13, and IL-17, and decreased the level of INF-γ (Fig. S4†). The levels of IL-4, IL-5, IL-13, and IL-17 were attenuated after the treatment with PEFF at all concentrations tested. In addition, the level of INF-γ was also increased by the

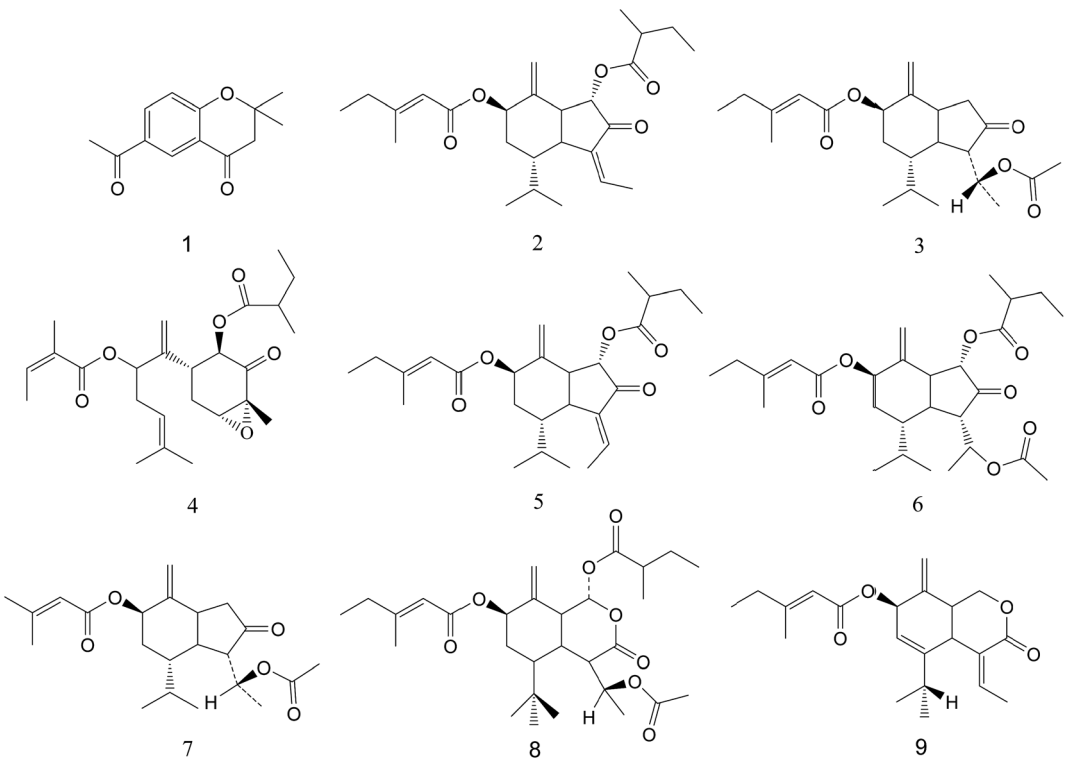

Fig. 2 The structures of compounds of PEFF.

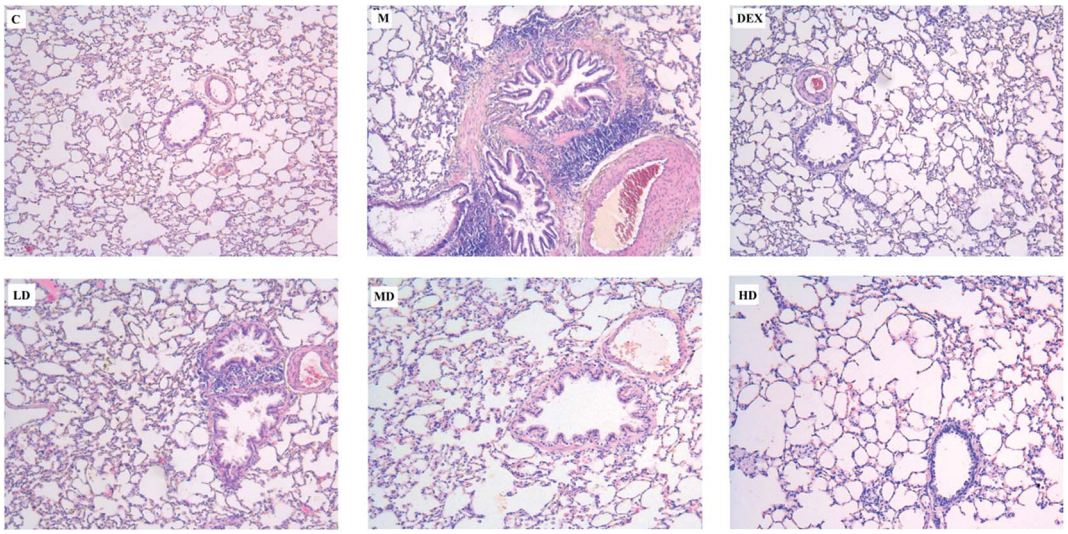

Fig. 3 Histopathological photomicrographs of rats lung, and C mean control group, M mean model group, DEX mean dexamethasone group, LD mean low dose group, MD mean middle dose group, and HD mean high dose group.

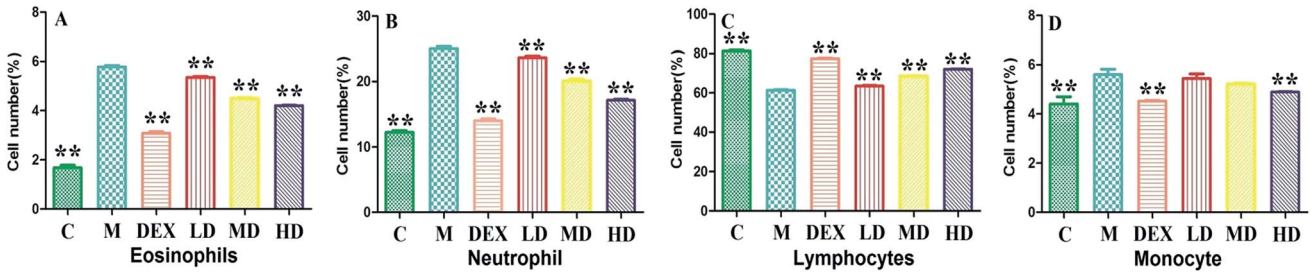

Fig. 4 Inflammatory cell counts in BALF of rats. The statistical significance of differences between model group and other groups ($n = 6$) are indicated as $p < 0.01$ (**).

treatment of PEFF. For these cytokines, the high dose group showed the best regulatory effect toward normal controls, and its regulatory effect was similar to that of DEX.

The rats in the model group showed significantly higher level of IgE ($p < 0.01$) in comparison to the control group, which could be reduced after treatments with PEFF at all of the tested doses. The HD group showed a significant ($p < 0.05$) reduction of about 30% in the IgE levels, and the regulatory effect was similar to that of DEX group (Fig. S4F†). In addition, the HO-1 content was found decreased in the rats sensitized and challenged with OVA (Fig. S4G†). After treatment with PEFF, the levels of HO-1 were strengthened at all of the tested doses ($p < 0.01$) as compared to the model group. It is worthy to note that the levels of HO-1 in all of the PEFF treated groups were higher than that in the DEX group.

3.5 Metabolomic study of rat lung

3.5.1 Multivariate data analysis of the lung extracts. The typical ^{1}H NMR spectra of the lung tissues of rats were shown in Fig. S5.† The spectral signals were assigned based on the chemical shifts of standard compounds from the literature data,[27] HMDB and BMRB database. The detected metabolites in the lung extracts and the corresponding NMR data were listed in ESI Table S3.†

To obtain more detailed metabolic differences between the control and model groups, the NMR data were subjected to multivariate data analysis. In the PCA score plot (Fig. S6A†), which were generated by PC1 (39.4%) and PC2 (12.7%), a clear separation could be observed between the control and OVA treated rats. To further maximize the difference between the control and model group, PLS-DA and OPLS-DA were also applied. The PLS-DA model was validated using the response of the permutation test through 200 permutations, in which all R^2 and Q^2 values were lower than the original ones, suggesting the validity of established discriminant model (Fig. S6B†). Thus, the metabolic difference did exist between the normal control and model group. For the OPLS-DA score plots (Fig. S6C†), the parameters R^2 (0.628), Q^2 (0.942), p values (2.03×10^{-4}) indicated the interpretability, predictability, as well as the validity of the established models. Then the corresponding S-plot (Fig. S6D†) combined with variable importance in the projection (VIP > 1.0) were applied to determine the metabolites contributing to the separation, which indicated that the rats in the model group showed higher levels of pyruvate, leucine, alanine, isoleucine,

valine, 3-hydroxybutyrate (3-HB), lysine, arginine, ornithine, acetate, glutamate, methionine, dimethylamine (DMA), creatine, phosphocholine (PC), phosphoethanolamine (PE), and scyllo-inositol, as well as lower levels of α-glucose, xanthine, hypoxanthine in the lung tissue, as compared with the normal controls.

3.5.2 Efficacy evaluation of PEFF by relative distance calculation and efficacy index. To reveal the drug action of PEFF, the PLS-DA score plot was depicted in Fig. 5, which exhibited obvious separation among the control, model, DEX, and PEFF (high dose, middle dose and low dose) groups. The DEX and PEFF groups were located between the control and model groups in the score plot, suggesting that PEFF could alter the perturbed metabolic profile caused by the OVA sensitization. In order to further evaluate the drug efficacy of PEFF quantitatively, the relative distances between treatment groups (model, DEX, HD, MD, LD) and control group in the PLS-DA (Fig. 5) score plot were calculated. The mean metabolic patterns of control group were used as the jumping-off point of metabolic pattern for other groups. The relative distances (Table 1) of all the drug-treated groups were smaller in comparison with the model group, and the relative distance of HD-treated group was smallest, indicating that the high dose of PEFF exerted the best effect against the OVA challenging.

In addition, relative integral levels of perturbed endogenous metabolites in the lung tissues of control, model and drug treated groups were listed in Fig. S7† for semi-quantitation. It is obviously that the contents of some perturbed metabolites in the lung tissues of PEFF treated groups were regulated toward normal state, indicating that the PEFF exerted the protective effect against the OVA sensitization.

Totally, the contents of 19 key metabolites (isoleucine, leucine, valine, 3-HB, lysine, alanine, arginine, ornithine, acetate, glutamate, methionine, pyruvate, DMA, creatine, PC, PE, scyllo-inositol, xanthine, hypoxanthine) could be reversed in treated-PEFF group of HD group. While 17 metabolites, including isoleucine, leucine, valine, 3-HB, lysine, ornithine, acetate, glutamate, methionine, pyruvate, DMA, creatine, PC, PE, α-glucose, xanthine, and hypoxanthine, could be reversed in the DEX group. Some of the metabolites, such as scyllo-inositol, alanine, arginine, could only be regulated by PEFF, while α-glucose could only be reversed in DEX group.

To further compare the drug efficacy, efficacy index, reflecting the integrated influence of the overall biomarkers, was introduced for quantification. The efficacy index of PEFF-treated rats in HD group was much higher than those of MD group and LD group (Table 2). In addition, the efficacy index of HD group was also higher than the DEX group, indicating that the high dose of PEFF exerted the best effect.

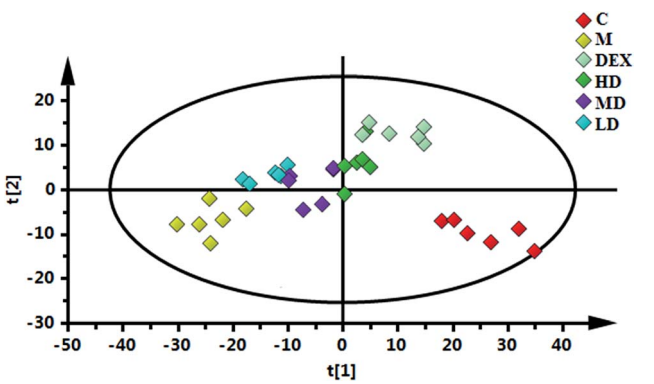

Fig. 5 PLS-DA score plots based on ^{1}H-NMR data of homogenates of rats, and C mean control group, M mean model group, DEX mean dexamethasone group, LD mean low dose group, MD mean middle dose group, and HD mean high dose group ($n = 6$).

Table 1 The relative distances among six groups of control, DEX and PEFF from the PLS-DA score of lung homogenates

	Control (mean)						
RD	*x*-axis	*y*-axis	DEX	HD	MD	LD	Model
	26.4249	−11.1433	28.941	29.164	34.296	39.669	40.513

3.6 Correlation analysis of biochemical indexes, and metabolites of *S*-plot

To investigate the relationship between the perturbed metabolites and biochemical indexes (IL-4, IL-5, IL-13, IL-17, IgE and IFN-γ), a correlation matrix was generated by calculating the Pearson's correlation coefficient. As shown in Fig. 6, IL-4 showed obviously positive correlations with glutamate, lysine, alanine, leucine, and methionine, and negative correlations with hypoxanthine, α-glucose, xanthine. A series of metabolites, including hypoxanthine, α-glucose, methionine, valine, isoleucine, and leucine, presented a higher correlation with IL-5. IL-13 had obviously positive correlations with methionine, pyruvate, valine, isoleucine, leucine, but negative correlations with hypoxanthine and α-glucose. Meanwhile, IL-17 had positive correlations with glutamate, acetate, ornithine, and lysine, and evidently negative correlations with hypoxanthine, xanthine and α-glucose. Besides, IFN-γ had correlations with the metabolites including 3-HB, DMA, glutamate, acetate, ornithine, hypoxanthine, evidently and lysine. IgE was positively correlated to glutamate and lysine, and was negatively correlated to hypoxanthine, xanthine and α-glucose. HO-1 showed obviously negative correlations with DMA, arginine and pyruvate.

3.7 PLS-RA analysis of potential biomarkers involved into OVA-induced asthma

PLS-RA was performed to gain possible relationships between the perturbed endogenous metabolites revealed by *S*-plot and biochemical indexes (IL-4, IL-5, IL-13, IL-17, IgE and IFN-γ). At first, the PLS-RA models were established, and the detailed diagnostic parameters of the models were shown in Table 3. Based on the model parameters (R^2X, Q^2Y, $Q^2Y > 0.5$, and P values <0.05) of PLS-RA, 13 metabolites, including pyruvate, leucine, alanine, isoleucine, valine, lysine, arginine, ornithine, acetate, glutamate, methionine, DMA and creatine, were found

Table 2 The efficacy index (%) of lung homogenates

No.	Integrals	Metabolites	DEX	HD	MD	LD
1	1.026–1.005	Isoleucine	68.49817	64.10256	38.46154	2.930403
2	0.982–0.949	Leucine	63.98446	63.09656	41.28746	14.76138
3	1.065–1.030	Valine	64.27221	63.138	36.67297	1.323251
4	1.215–1.196	3-HB	87.57764	82.6087	63.97516	62.1118
6	1.742–1.718	Lysine	67.69706	64.45131	43.43122	0.309119
7	1.500–1.470	Alanine	88.18681	187.6374	180.4945	440.3846
8	1.713–1.694	Arginine	460.5744	83.28982	77.54569	17.49347
9	1.766–1.743	Ornithine	88.66856	78.18697	69.68839	35.97734
10	1.935–1.917	Acetate	83.27444	80.68316	55.7126	29.44641
11	2.072–2.035	Glutamate	63.97749	51.78236	31.70732	9.287054
12	2.150–2.134	Methionine	60.16129	50.96774	28.06452	3.225806
17	2.368–2.376	Pyruvate	27.31959	55.15464	38.14433	13.91753
19	2.727–2.716	DMA	91.66667	81.94444	76.38889	65.27778
21	3.946–3.930	Creatine	73.9508	61.21563	23.29957	8.972504
24	3.621–3.611	PC	42.33577	37.59124	26.27737	18.24818
25	3.279–3.267	PE	246.2963	1175.926	772.2222	761.1111
28	3.374–3.358	Scyllo-inositol	93.10345	76.72414	13.7931	18.10345
33	5.262–5.230	α-glucose	143.4109	74.4186	48.83721	1.550388
40	7.937–7.900	Xanthine	146.087	84.34783	50.43478	4.347826
41	8.233–8.190	Hypoxanthine	98.39572	82.8877	79.67914	67.37968
Efficacy index (EI)			2159.439	2600.155	1796.118	1576.159

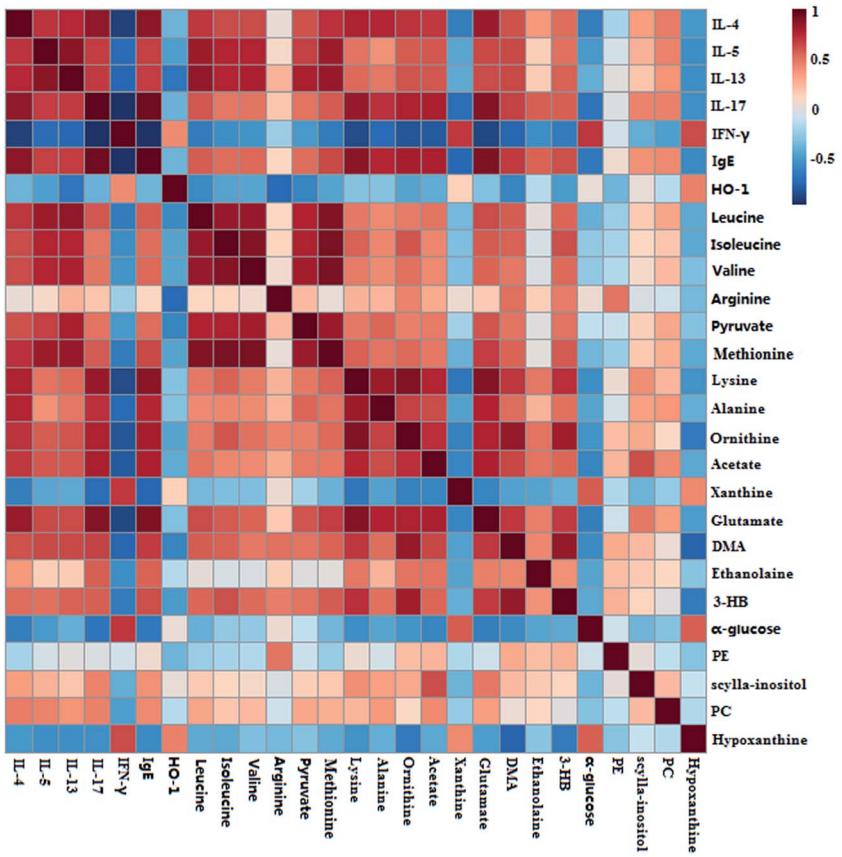

Fig. 6 Pearson's correlations analysis of biochemical indexes, and metabolites of *S*-plot from lung samples.

closed related with the levels change of the biochemical indexes (Table 3), and after the treatment of PEFF, all of these 13 altered metabolites were regulated toward normal controls.

3.8 Molecular docking analysis

In order to explore the active ingredients in PEFF that have efficacy in asthma, molecular docking analysis was also

Table 3 Summary of the PLS-RA models diagnostic parameters

No.	Metabolites	R^2X^a	R^2Y^a	Q^2Y^b	p value^c
1	Isoleucine	0.887	0.632	0.565	2.86×10^{-5}
2	Leucine	0.898	0.758	0.727	3.022×10^{-8}
3	Valine	0.968	0.670	0.625	4.44×10^{-5}
4	3-HB	0.759	0.424	0.347	8.73×10^{-4}
6	Lysine	0.969	0.710	0.661	1.26×10^{-5}
7	Alanine	0.895	0.553	0.502	2.18×10^{-4}
8	Arginine	0.969	0.634	0.592	1.55×10^{-4}
9	Ornithine	0.902	0.659	0.603	7.73×10^{-6}
10	Acetate	0.896	0.626	0.585	1.28×10^{-5}
11	Glutamate	0.867	0.757	0.712	6.05×10^{-8}
12	Methionine	0.968	0.768	0.734	4.74×10^{-7}
17	Pyruvate	0.907	0.625	0.584	1.39×10^{-5}
19	DMA	0.908	0.637	0.561	3.38×10^{-5}
21	Creatine	0.869	0.582	0.501	2.12×10^{-4}
24	PC	0.762	0.218	0.057	0.378
25	PE	0.228	0.326	0.184	0.348
28	Scyllo-inositol	0.759	0.115	0.700	0.307
33	α-glucose	0.826	0.541	0.458	7.35×10^{-4}
40	Xanthine	0.869	0.414	0.367	5.63×10^{-3}
41	Hypoxanthine	0.758	0.392	0.336	1.16×10^{-3}

[a] R^2X and R^2Y are cumulative modeled variation in the X and the Y matrix, respectively. [b] Q^2Y is the cumulative predicted variation in the Y matrix. [c] p-value, obtained from cross validation ANOVA of the PLS-RA models.

Table 4 The docking scores of 9 active ingredients and its targets in PEFF

No.	Target gene	PDB ID	Docking score
1	IL-17	5HI4	6.066
	IL-13	5L6Y	5.823
2	IL-17	5HI4	6.69
	IL-13	5L6Y	5.142
	IgE	5LGK	5.135
3	IL-17	5HI4	6.701
	IL-13	5L6Y	5.43
	IgE	5LGK	5.275
4	IL-17	5HI4	6.712
	IL-13	5L6Y	6.482
5	IL-17	5HI4	6.693
	IL-13	5L6Y	6.662
	IgE	5LGK	5.113
6	IL-17	5HI4	6.644
	IL-13	5L6Y	5.276
	IgE	5LGK	5.109
7	IL-17	5HI4	6.763
	IL-13	5L6Y	5.275
	IgE	5LGK	5.157
8	IL-17	5HI4	6.708
	IL-13	5L6Y	5.343
	IgE	5LGK	5.154
9	IL-17	5HI4	6.708
	IL-13	5L6Y	5.054
	IgE	5LGK	5.067

performed. The biochemical indexes (IL-4, IL-5, IL-13, IL-17, IgE and IFN-γ) were imported into RCSB Protein Data Bank (http://www.rcsb.org/pdb/), and then the corresponding IDs could be found. Then the PDB IDs of the biochemical indexes and 9 compounds identified in PEFF, were imported into systems dock (http://systemsdock.unit.oist.jp/). Based on molecular docking, the tight binding of active ingredients with potential protein targets with the docking score (>4.52)[28] were filtered out as the tightest binding ligand, and the scores were tabulated in Table 4.

The nine compounds identified in PEFF were found to bound with different protein targets. Among the tested protein targets, IL-13 and IL-17 showed high docking scores with the nine compounds, implying that these components in PEFF were effective for asthma by regulating the cytokines of IL-13 and IL-17. The results further proved that the IL-13 and IL-17 did play a direct role in asthma. In addition, seven compounds (2, 3, 5, 6, 7, 8, 9) exhibited tight docking to the IgE, which suggested that some compounds in PEFF were also effective by directly affecting the IgE.

4. Discussion

4.1 Inflammation analysis in BALF

The OVA-induced lung inflammation in rats, resulted in a Th2-type response with a significant increase of monocyte, particularly eosinophils and neutrophils, into the lung tissue.[29] The eosinophilia in asthmatic patients is a key hallmark of asthma and correlates with severe exacerbations. Eosinophils can lead to bronchoconstriction, mucus secretion, and structural damage to the pulmonary region, with bronchial hyperresponsiveness.[30] In this study, the influx of inflammatory cells into the airways were reduced significantly after the treatment of PEFF, and the effect was close to that of DEX. The results of histological analysis also confirmed the effect of PEFF on the cell migration.

4.2 Biochemical indexes analysis

The cytokines secreted by Thl cells can promote cellular immune response to asthma, which shows a protective effect against asthma. The factors of Th2 cells can affect T cell differentiation in the onset of asthma and airway inflammation.[31] IL-4, IL-5 and IL-13, which are secreted by Th2 lymphocytes, can stimulate IgE production and are also associated with the development and malignant outcome of pulmonary fibrosis. In addition, IL-5 has been demonstrated to play a key role in the maturation of eosinophils,[32] such that the generation of eosinophils is suppressed if the production of IL-5 is inhibited. IFN-γ produced by Th1 cells, shows an inhibitory action on IgE production.[33] The above mentioned cytokines in asthmatic rats were investigated after the treatment of PEFF, and the results indicated that the high and middle dose of PEFF, as well as DEX could reduce the serum levels of IL-4, IL-5, IL-13 as well as IgE significantly. The results presented here suggested that PEFF could suppress IgE secretion by reducing the production of IL-4, IL-5 and IL-13, which, in turn, could suppress the maturation of eosinophils and reduce the IgE in the serum, thus alleviating inflammation and asthma. In addition, the levels of IFN-γ in the DEX and PEFF treatment

groups were increased compared with the model group. The above mentioned results suggested that the anti-asthmatic effect of PEFF was probably related with the balancing of the Th1/Th2 cells.

IL-17 is a cytokine that has been reported to be produced by Th17 cells. In a recent study, Molet *et al.*[34] demonstrated that the eosinophils was the cellular source of the production of IL-17, which was up-regulated in asthma. Chabaud *et al.*[35] evidenced that IL-17 play an indirect role in airway remodeling in asthma. The increased expression of IL-17 in OVA-induced asthmatic rats could be reduced significantly by the treatment of PEFF, indicated that the action of PEFF on asthmatic rats was also related with the regulation of IL-17. HO-1 is a rate-limiting enzyme of ferroprotoporphyrin metabolism, and it is a stress-induced protein. HO-1 catalyzes ferroprotoporphyrin to generate biliverdin, bilirubin, and CO. These enzymatic products are responsible for HO-1 action.[36] HO-1 exerts a protective effect for tissue injury through multiple mechanisms including anti-oxidation, anti-inflammation, and anti-apoptosis. The anti-inflammatory effect of HO-1 has been well studied in respiratory diseases. In several airway inflammatory models, HO-1 is found to reduce local inflammatory cell infiltration.[37] In addition, HO-1 can stabilize mast cells, lessen IgE production, and inhibit adhesion molecules.[38] Therefore, HO-1 plays an important role in preventing airway inflammation. Previous studies showed that the anti-inflammatory effect of sesquiterpnenoids was mideated by Nrf2/HO-1 pathway.[39] Compared with model group, the serum HO-1 level was increased remarkably after the treatment with PEFF, suggesting that the anti-asthmatic effect of PEFF was also involved with anti-inflammatory effect by Nrf2/HO-1 regulation.

4.3 Metabolic pathways analysis

In order to explore the possible pathways that were affected by PEFF, differential biomarkers that had correlation with biochemical indexes (IL-4, IL-5, IL-13, IL-17, IFN-γ, IgE and HO-1) were imported into MetaboAnalyst. Three metabolic pathways, including arginine and proline metabolism, pyruvate metabolism, D-glutamine and D-glutamate metabolism, with the impact-value >0.1 were filtered out as the most important metabolic pathways, and mapped on KEGG for the host response to PEFF (Fig. S8†).[40] These metabolic changes and the associated pathways provided deep insights into the mechanism of anti-asthmatic effect of PEFF (Fig. S8†).

Arginine is one of the most versatile amino acids in animal cells, serving as a precursor for the synthesis of not only proteins but also nitric oxide, urea, polyamines, proline, glutamate, creatine and agmatine. Arginine can regulate the immunity system by means of arginase and nitric oxide metabolic pathways as an immune regulator.[41] Metabolism of proline could generate electrons to produce ROS and initiate a variety of downstream effects, including blockade of the cell cycle, autophagy and apoptosis.[42] Thus, the metabolites of arginine and proline were closely related to the progression of oxidative stress. In this study, the increase arginine was reduced after the treatment of PEFF, suggesting the anti-asthmatic effect of PEFF was probably related with the inhibition of ROS generation.

Pyruvate, an important intermediate product of glycolysis, can be used to produce acetyl-CoA by pyruvate dehydrogenase complex. Acetyl-CoA could enter into the TCA cycle, and plays a key role in the glucose aerobic oxidation and energy production.[43] The increased level of pyruvate indicated the inhibition of aerobic respiration in OVA-induced rats. Compared with the model group, the level of pyruvate was decreased in the lung of PEFF-treated rats, suggesting the recovery of aerobic respiration.

Several studies outlined that glutamine is essentially involved in the inter-organ nitrogen transportation, however, high concentration of glutamate could cause excessive stimulation of glutamate receptors and lead to neurotoxicity.[44] Previous studies also showed that the serum glutamine was increased in the asthma patients.[45] In this study, the glutamine and glutamate were increased in the OVA challenged rats, and decreased after PEFF treatment, suggesting the protective effect of PEFF against asthma was also related with the regulation of glutamine and glutamate metabolism.

5. Conclusion

A ^{1}H NMR based metabolomics approach coupled with biochemical assay and histopathological inspection had been employed to study the protective effect of PEFF against OVA-induced asthma using rats model. The metabolic perturbation in the lung extracts were characterized by the levels increase of pyruvate, leucine, isoleucine, valine, 3-HB, lysine, alanine, arginine, ornithine, acetate, glutamate, methionine, DMA, creatine, PC, PE, and scyllo-inositol, as well as levels decrease of α-glucose, xanthine, hypoxanthine. Among the perturbed metabolites, 19 of them could be reversed by PEFF, and the MetPA analysis revealed that the anti-asthamtic effect of PEFF was probably related with regulation of arginine and proline metabolism, pyruvate metabolism, D-glutamine and D-glutamate metabolism. The regulatory effects on the cytokines (IL-4, IL-5, IL-13, and IL-17) and serum HO-1 level suggested that the anti-asthmatic action of PEFF were probably related with the balancing of the Th1/Th2 cells and the Nrf2/HO-1 pathway.

The results of chemical analysis showed that the sesquiterpenes were present as the major components in PEFF, and molecular docking analysis suggested that these compounds showed high docking scores with cytokines of IL-13, IL-17 and IgE, suggesting that these compounds in PEFF maybe relate with its anti-asthmatic effect. However, further studies are needed to validate the active compounds in PEFF. In addition, whether the synergistic effect exists among these compounds should also be investigated.

Conflict of interest

We confirm that this manuscript has not been published by another journal. All authors have approved the manuscript and agree with its submission to your journal. The authors declare that there is no conflict of interests regarding the publication of this paper.

Ethics statement

All experiments in this study were in accordance with NIH Guide for the Care and Use of Laboratory Animals, and approved by institutional ethical committee of Shanxi University. Maximum efforts were made to minimize animal suffering and the number of animals necessary for the capture of reliable data.

Acknowledgements

This study was financially supported by the National Natural Science Foundation of China (No. 31270008), National Standardization Program of Traditional Chinese Medicine (No. ZYBZH-Y-JIN-34); Program for the Outstanding Innovative Teams of Higher Learning Institutions of Shanxi (OIT), Key Laboratory of Effective Substances Research and Utilization in TCM of Shanxi Province (201605D111004), and Science and technology innovation team of Shanxi Province (201605D131045-18), The Key Scientific and Technological Innovation Platform Foundation for Head and Neck Cancer Research of Shanxi Province (201605D151003), The Scientific and Technological Achievements Transformation Guidance Foundation of Shanxi Province (201604D1-31002). We also thank Scientific Instrument Center of Shanxi University for the NMR analysis.

References

1 Global Initiavite for Asthma, Global strategy for asthma management and prevention 2014 (2014), available from: http://www.ginasthma.org, accessed 4th December 2015.
2 T. F. Gajewski, J. Joyce and F. W. Fitch, Antiproliferative effect of IFN-gamma in immune regulation. III. Differential selection of TH1 and TH2 murine helper T lymphocyte clones using recombinant IL-2 and recombinant IFN-gamma, *J. Immunol.*, 1989, **143**, 15–22.
3 O. Nagashima, N. Harada, Y. Usui, *et al.*, B7-H3 contributes to the development of pathogenic Th2 cells in a murine model of asthma, *J. Immunol.*, 2008, **181**, 4062–4071.
4 Y. Endo, K. Hirahara, R. Yagi, *et al.*, Pathogenic memory type Th2 cells in allergic inflammation, *Trends Immunol.*, 2014, **35**, 69–78.
5 K. Oeser, J. Maxeiner, C. Symowski, M. Stassen, *et al.*, T cells are the critical source of IL-4/IL-13 in a mouse model of allergic asthma, *Allergy*, 2015, **70**, 1140–1149.
6 E. Sarnes, L. Crofford, M. Watson, *et al.*, Incidence and US costs of corticosteroid-associated adverse events: a systematic literature review, *Clin. Ther.*, 2011, **33**, 1413–1432.
7 P. G. Woodruff, H. A. Boushey, G. M. Dolganov, *et al.*, Genome-wide profiling identifies epithelial cell genes associated with asthma and with treatment response to corticosteroids, *Proc. Natl. Acad. Sci. U. S. A.*, 2007, **104**, 15858–15863.
8 K. Mattishent, M. Thavarajah, P. Blanco, *et al.*, Meta-review: adverse effects of inhaled corticosteroids relevant to older patients, *Drugs*, 2014, **74**, 539–547.
9 C. Huang, W. Li, B. Wu, *et al.*, Pheretima aspergillum decoction suppresses inflammation and relieves asthma in a mouse model of bronchial asthma by NF-κB inhibition, *J. Ethnopharmacol.*, 2016, **189**, 22–30.
10 F. M. de, B. C. Azevedo, F. Carmona, *et al.*, A standardized methanol extract of Eclipta prostrata (L.) L. (Asteraceae) reduces bronchial hyperresponsiveness and production of Th2 cytokines in a murine model of asthma, *J. Ethnopharmacol.*, 2017, **198**, 226–234.
11 D. A. T. de Almeida, S. I. G. Rosa, T. C. D. da Cruz, *et al.*, Mandevilla longiflora (Desf.) Pichon improves airway inflammation in a murine model of allergic asthma, *J. Ethnopharmacol.*, 2017, **200**, 51–59.
12 M. F. P. Corrêa, G. O. de Melo, S. S. Costa, *et al.*, Substâncias de origem vegetal potencialmente úteis na terapia da Asma, *Dados*, 2008, **18**, 785–797.
13 C. P. Commission, *Pharmacopoeia of the People's Republic of China*, China Medical Science Press, Beijing, 2015, vol. 1, p. 332.
14 C. Hwangbo, H. S. Lee, J. Park, *et al.*, The anti-inflammatory effect of tussilagone, from Tussilago farfara, is mediated by the induction of heme oxygenase-1 in murine macrophages, *Int. Immunopharmacol.*, 2009, **9**, 1578–1584.
15 H. Li, H. J. Lee, *et al.*, Tussiabone suppresses colon cancer cell proliferation by promoting the degradation of β-catenin, *Biochem. Biophys. Res. Commun.*, 2014, **443**, 132–137.
16 H. J. Lim, H. S. Lee and J. H. Ryu, Suppression of inducible nitric oxide synthase and yclooxygenase-2 expression by tussilagone from Farfarae Flos in BV-2 microglial cells, *Arch. Pharmacal Res.*, 2008, **31**, 645–652.
17 W. Shi and G. Q. Han, Chemical constituents of *tussilago farfara* L., *J. Chin. Pharm. Sci.*, 1996, **5**, 63–67.
18 H. Gao, Y. N. Huang, B. Gao, *et al.*, α-Glucosidase inhibitory effect by the flower buds of Tussilago farfara L., *Food Chem.*, 2008, **106**, 1195–1201.
19 M. R. Kim, J. Y. Lee, H. H. Lee, *et al.*, Antioxidative effects of quercetin-glycosides isolated from the flower buds of Tussilago farfara L., *Food Chem. Toxicol.*, 2006, **44**, 1299–1307.
20 J. O. Santer and R. Stevenson, Arnidiol and faradiol, *J. Org. Chem.*, 1962, **27**, 3204–3208.
21 J. H. Ryu, Y. S. Jeong and D. H. Sohn, A new bisabolene epoxide from Tussilago farfara and inhibition of nitric oxide synthesis in LPS-activated macrophages, *J. Nat. Prod.*, 1999, **62**, 1437–1438.
22 Z. Jiang, F. Liu, J. J. L. Goh, *et al.*, Determination of senkirkine and senecionine in *Tussilago farfara* using microwave-assisted extraction and pressurized hot water extraction with liquid chromatography tandem mass spectrometry, *Talanta*, 2009, **79**, 539–546.
23 X. Fei, X. Zhang, G. Zhang, *et al.*, Cordycepin inhibits airway remodeling in a rat model of chronic asthma, *Biomed. Pharmacother.*, 2017, **88**, 335–341.
24 X. Huang, L. Shao, Y. Gong, *et al.*, A metabonomic characterization of CCl4-induced acute liver failure using partial least square regression based on the GC/MS metabolic profiles of plasma in mice, *J. Chromatogr. B: Anal. Technol. Biomed. Life Sci.*, 2008, **870**, 178–185.

25 J. K. Nicholson, P. J. Foxall, M. Spraul, *et al.*, Lindon, 750 MHz ^{1}H and ^{1}H-^{13}C NMR spectroscopy of human blood plasma, *Anal. Chem.*, 1995, **67**, 793–811.
26 N. Psychogios, D. D. Hau, J. Peng, *et al.*, The human serum metabolome, *PLoS One*, 2011, **6**, e16957.
27 A. P. Li, Z. Y. Li, H. F. Sun, *et al.*, Comparison of two different Astragali radix by a ^{1}H NMR-based metabolomic approach, *J. Proteome Res.*, 2015, **14**, 2005–2016.
28 K. Y. Hsin, S. Ghosh and H. Kitano, Combining machine learning systems and multiple docking simulation packages to improve docking prediction reliability for network pharmacology, *PLoS One*, 2013, **8**, e83922.
29 R. K. Kumar, C. Herbert and P. S. Foster, The "classical" ovalbumin challenge model of asthma in mice, *Curr. Drug Targets*, 2008, **9**, 485–494.
30 A. J. Wardlaw, C. Brightling, R. Green, *et al.*, Eosinophils in asthma and other allergic diseases, *Br. Med. Bull.*, 2000, **56**, 985–1003.
31 F. K. Gibbons, E. Israel, A. Deykin, *et al.*, The combined effects of zafirlukast, prednisone, and inhaled budesonide on IL-13 and IFN-γ secretion, *J. Clin. Immunol.*, 2005, **25**, 437–444.
32 A. P. Sampson, IL-5 priming of eosinophil function in asthma, *Clin. Exp. Allergy*, 2001, **31**, 513–517.
33 Y. Endo, K. Hirahara, R. Yagi, D. J. Tumes, *et al.*, Pathogenic memory type Th2 cells in allergic inflammation, *Trends Immunol.*, 2014, **35**, 69–78.
34 S. Molet, Q. Hamid, F. Davoineb, *et al.*, IL-17 is increased in asthmatic airways and induces human bronchial fibroblasts to produce cytokines, *J. Allergy Clin. Immunol.*, 2001, **108**, 430–438.
35 M. Chabaud, F. Fossiez, J. L. Taupin, *et al.*, Enhancing effect of IL-17 on IL-1-induced IL-6 and leukemia inhibitory factor production by rheumatoid arthritis synoviocytes and its regulation by Th2 cytokines, *J. Immunol.*, 1998, **161**, 409–414.
36 L. E. Otterbein, F. H. Bach, J. Alam, *et al.*, Carbon monoxide has anti-inflammatory effects involving the mitogen-activated protein kinase pathway, *Nat. Med.*, 2000, **6**, 422–428.
37 J. K. Sarady, S. L. Otterbein, F. Liu, *et al.*, Carbon monoxide modulates endotoxin-induced production of granulocyte macrophage colony-stimulating factor in macrophages, *Am. J. Respir. Cell Mol. Biol.*, 2002, **27**, 739–745.
38 R. Song, R. S. Mahidhara, F. Liu, *et al.*, Carbon monoxide inhibits human airway smooth muscle cell proliferation *via* mitogen-activated protein kinase pathway, *Am. J. Respir. Cell Mol. Biol.*, 2002, **27**, 603–610.
39 J. Lee, U. Kang, E. K. Seo, *et al.*, Heme oxygenase-1-mediated anti-inflammatory effects of tussilagonone on macrophages and 12-O-tetradecanoylphorbol-13-acetate-induced skin inflammation in mice, *Int. Immunopharmacol.*, 2016, **34**, 155–164.
40 X. Wang, B. Yang, H. Sun, *et al.*, Pattern recognition approaches and computational systems tools for ultra performance liquid chromatography-mass spectrometry-based comprehensive metabolomic profiling and pathways analysis of biological data sets, *Anal. Chem.*, 2011, **84**, 428–439.
41 W. U. Guoyao and S. M. Morris, Arginine metabolism: nitric oxide and beyond, *Biochem. J.*, 1998, **336**, 1–17.
42 J. M. Phang, W. Liu and O. Zabirnyk, Proline metabolism and microenvironmental stress, *Annu. Rev. Nutr.*, 2010, **30**, 441–463.
43 B. Plecko, S. Stoeckler-Ipsiroglu, E. Schober, *et al.*, Oral β-hydroxybutyrate supplementation in two patients with hyperinsulinemic hypoglycemia: Monitoring of β-hydroxybutyrate levels in blood and cerebrospinal fluid, and in the brain by *in vivo* magnetic resonance spectroscopy, *Pediatr. Res.*, 2002, **52**, 301–306.
44 A. Kumar, R. L. Singh and G. N. Babu, Cell death mechanisms in the early stages of acute glutamate neurotoxicity, *Neurosci. Res.*, 2010, **66**, 271–278.
45 J. Jung, S. H. Kim, H. S. Lee, *et al.*, Serum metabolomics reveals pathways and biomarkers associated with asthma pathogenesis, *Clin. Exp. Allergy*, 2013, **43**, 425–433.